

A hybrid kinetic WENO scheme for compressible flow simulations

Hongwei Liu*, Changping Yu, Xinliang Li

*Corresponding author: hliu@imech.ac.cn

State Key Laboratory of High Temperature Gas Dynamics, Institute of Mechanics,
Chinese Academy of Sciences, Beijing, China

Abstract: The hybrid kinetic Weighted Essentially Non-Oscillatory (WENO) scheme proposed in *Int. J. Numer. Meth. Fluids* 2015, 79: 290-305 is further studied in this paper. In a conventional WENO framework, flux vector splitting (FVS) techniques are usually used for the numerical flux evaluation at cell interfaces, and it is well known that the numerical dissipation of FVS methods is relatively large due to the free transfer mechanism of gas molecules, in order to reduce the dissipation in the procedure of flux calculations, a hybrid kinetic WENO scheme was introduced in the above-mentioned paper, where the 5th order scheme employing the proposed hybrid kinetic approach has been validated. In this paper, we further test the 7th order scheme using the hybrid kinetic method. It is indicated that the 7th order hybrid kinetic WENO scheme is more accurate and less dissipative than that adopting conventional FVS techniques and has a good shock-capturing capability, some examples including both one-dimensional and two-dimensional cases are presented.

Keywords: Gas Kinetic Theory, WENO Method, Hybrid Numerical Flux, Numerical Dissipation.

1 Introduction

Essentially Non-Oscillatory (ENO) schemes were started with the classic paper of Harten et al.[1] and further efficiently implemented in [2, 3] for hyperbolic conservation laws. Later Weighted ENO (WENO) schemes were developed [4, 5], using a convex combination of all candidate stencils instead of just one as in the original ENO idea. The WENO reconstruction is very effective in both controlling numerical oscillations and restoring smooth distributions, which has been widely used in many practical applications.

In recent years, the development of gas-kinetic schemes for compressible flow simulations has attracted much attention and become mature, such as the Kinetic Flux Vector Splitting (KFVS) methods[6, 7, 8], the various algorithms based on the Bhatnagar-Gross-Krook (BGK) model[9, 10, 11, 12, 13], and many others. The gas-kinetic schemes use various kinetic equations to model the dynamic processes around a cell interface and can provide robust and accurate numerical solutions for various compressible flows.

The combination of the WENO reconstruction and gas-kinetic flux formulation has been recently studied by some researchers [14, 15, 16]. In [24], a hybrid kinetic WENO scheme was proposed based on the hybridization of two types of kinetic fluxes, i.e. the free transfer KFVS flux and the collision-related flux, both evaluated from the WENO reconstruction technique. The 5th order scheme employing the proposed hybrid kinetic approach has been validated in [24]. In this paper, we will

further test the 7th order scheme using the hybrid kinetic method. It is indicated that the 7th order hybrid kinetic WENO scheme is more accurate and less dissipative than that adopting conventional FVS techniques and has a good shock-capturing capability, many examples including both one-dimensional and two-dimensional cases will be presented.

2 Hybrid kinetic WENO scheme

The finite volume hybrid kinetic WENO scheme proposed in [24] will be briefly presented in this section. The WENO reconstruction techniques proposed in [5, 25] will be used in the proposed hybrid kinetic scheme. Some improved smoothness indicators have been proposed and investigated recently[17, 18, 19], our numerical experiments indicate that these smoothness indicators can also work well for the proposed scheme.

Next we will describe the hybrid kinetic WENO scheme [24] for solving the Euler equations. For the sake of simplicity, only the one-dimensional case is presented and it can be easily extended to multidimensional cases in a dimension by dimension manner [5]. The 1D Euler equations can be written as

$$\frac{\partial \mathbf{U}}{\partial t} + \frac{\partial \mathbf{F}(\mathbf{U})}{\partial x} = 0, \quad (1)$$

where $\mathbf{U} = (\rho, \rho u, E)^T$ and \mathbf{F} is given by $\mathbf{F} = (\rho u, \rho u^2 + p, u(E + p))^T$. For a uniform grid with the cell center x_i , the cell interface $x_{i+1/2}$ and the cell size Δx , a finite volume method can be written as

$$\frac{d\bar{\mathbf{U}}_i}{dt} = -\frac{1}{\Delta x} (\hat{\mathbf{F}}_{i+1/2} - \hat{\mathbf{F}}_{i-1/2}). \quad (2)$$

The third-order TVD Runge-Kutta method proposed in [2] will be used to integrate in time. Therefore we only need to specify the construction of the numerical flux $\hat{\mathbf{F}}_{i+1/2}$ for a finite volume scheme.

2.1 Conventional WENO scheme

As shown in [5], the numerical flux $\hat{\mathbf{F}}_{i+1/2}$ in Eq. (2) can be divided into two parts

$$\hat{\mathbf{F}}_{i+1/2} = \hat{\mathbf{F}}_{i+1/2}^+ + \hat{\mathbf{F}}_{i+1/2}^-, \quad (3)$$

where $\hat{\mathbf{F}}_{i+1/2}^+$ is the flux along x-positive direction and $\hat{\mathbf{F}}_{i+1/2}^-$ is the flux along x-negative direction. Let $\bar{\mathbf{F}}_i$ be the numerical flux based on the cell averaged value $\bar{\mathbf{U}}_i$. In order to evaluate $\hat{\mathbf{F}}_{i+1/2}^\pm$ in Eq. (3), first we split the numerical flux into two parts

$$\bar{\mathbf{F}}_i = \bar{\mathbf{F}}_i^+ + \bar{\mathbf{F}}_i^-, \quad (4)$$

which can be achieved by many flux splitting approaches, such as the Lax-Friedrichs [5] or Steger-Warming[20] flux splitting method. Then the numerical flux $\hat{\mathbf{F}}_{i+1/2}^+$ in Eq. (3) can be obtained from $\bar{\mathbf{F}}_i^+$ by the WENO reconstruction technique, and $\hat{\mathbf{F}}_{i+1/2}^-$ can be calculated from $\bar{\mathbf{F}}_i^-$ by a symmetric procedure with respect to $x_{i+1/2}$. The underlying physical principle for such a conventional WENO algorithm is the collisionless free transfer of gas molecules.

The kinetic flux vector splitting (KFVS) technique [6, 7] can also be used in Eq. (4), and the numerical flux $\hat{\mathbf{F}}_{i+1/2}$ in Eq. (3) calculated by the KFVS approach is denoted by $\hat{\mathbf{F}}_{i+1/2}^{\text{KFVS}}$, and a conventional 5th-order/7th-order WENO algorithm[5, 25] based on the KFVS technique will be called the W5-KFVS/W7-KFVS scheme hereafter in this paper.

2.2 Hybrid kinetic WENO scheme

In the following we will present the construction of a hybrid kinetic numerical flux, which includes the effects of both the free transfer and the collision of gas molecules. The hybrid kinetic flux can be written as

$$\hat{\mathbf{F}}_{i+1/2} = \alpha \hat{\mathbf{F}}_{i+1/2}^{\text{KFVS}} + (1-\alpha) \hat{\mathbf{F}}_{i+1/2}^{\text{C}}, \quad (5)$$

where $\hat{\mathbf{F}}_{i+1/2}^{\text{KFVS}}$ is the collisionless KFVS-type numerical flux, $\hat{\mathbf{F}}_{i+1/2}^{\text{C}}$ is the numerical flux due to molecule collision effects, and α is a parameter in the range $0 \leq \alpha \leq 1$ and will be hereafter called the jump indicator. It should be pointed out that this kind of hybrid numerical fluxes has been used in some kinetic schemes, see for example [21, 22, 23], and to name just a few.

Since the evaluation of the collisionless KFVS-type flux $\hat{\mathbf{F}}_{i+1/2}^{\text{KFVS}}$ in Eq. (5) is the same as that described in the preceding subsection, therefore in order to use Eq. (5) to get the hybrid numerical flux, we only need to determine the collision-related kinetic flux $\hat{\mathbf{F}}_{i+1/2}^{\text{C}}$ and the jump indicator α .

The collision-related kinetic flux $\hat{\mathbf{F}}_{i+1/2}^{\text{C}}$ can be constructed as follows. The basic idea of evaluating is to calculate the flux $\hat{\mathbf{F}}_{i+1/2}^{\text{C}}$ based on the collision-related state $\hat{\mathbf{U}}_{i+1/2}^{\text{C}}$ constructed at the cell interface $x_{i+1/2}$. In order to get the collision-related state, first we split the cell averaged conservative variable $\bar{\mathbf{U}}_i$ into two parts

$$\bar{\mathbf{U}}_i = \bar{\mathbf{U}}_i^+ + \bar{\mathbf{U}}_i^-, \quad (6)$$

where

$$\left. \begin{aligned} \bar{\mathbf{U}}_i^+ &= \int_{R^k} \int_{v>0} \psi g(\bar{\mathbf{U}}_i, v, \xi) dv d\xi \\ \bar{\mathbf{U}}_i^- &= \int_{R^k} \int_{v<0} \psi g(\bar{\mathbf{U}}_i, v, \xi) dv d\xi \end{aligned} \right\}. \quad (7)$$

Then the collision-related state $\hat{\mathbf{U}}_{i+1/2}^{\text{C}}$ at the cell interface can be obtained by

$$\hat{\mathbf{U}}_{i+1/2}^{\text{C}} = \hat{\mathbf{U}}_{i+1/2}^+ + \hat{\mathbf{U}}_{i+1/2}^-, \quad (8)$$

where $\hat{\mathbf{U}}_{i+1/2}^+$ is determined from $\bar{\mathbf{U}}_i^+$ by the WENO reconstruction technique, and $\hat{\mathbf{U}}_{i+1/2}^-$ is calculated from $\bar{\mathbf{U}}_i^-$ by a symmetric procedure with respect to $x_{i+1/2}$.

The principle to construct the jump indicator α is that the contribution of the flux $\hat{\mathbf{F}}_{i+1/2}^{\text{KFVS}}$ should be dominant around strong shock waves and small in smooth regions. This is because that the collisionless flux $\hat{\mathbf{F}}_{i+1/2}^{\text{KFVS}}$ is more dissipative than the collision-related flux $\hat{\mathbf{F}}_{i+1/2}^{\text{C}}$. Similar to the way in [21, 22, 23], in the present study we use the local pressure jump around the cell interface to determine the jump indicator α ,

$$\alpha = 1 - \exp\left(-C \frac{|\bar{p}_{i+1} - \bar{p}_i|}{\bar{p}_{i+1} + \bar{p}_i}\right), \quad (9)$$

where C is an empirical positive constant, it can be seen that for the same local pressure jump, a larger value of C results in a larger value of α and therefore more KFVS-type contribution in the hybrid kinetic flux which makes the scheme more dissipative. Fortunately, our numerical experiments as well as those in [21, 22, 23] indicate that the numerical results are not sensitive to the chosen value of C , for the present hybrid kinetic scheme, we find that $C=10$ is a quite good choice based on plenty of numerical experiments, therefore it is used for all the numerical tests in this paper, and the same value of C has been adopted in [22].

From Eq. (5) we can see that both $\hat{\mathbf{F}}_{i+1/2}^{\text{KFVS}}$ and $\hat{\mathbf{F}}_{i+1/2}^{\text{C}}$ need to be calculated for each cell interface except for $\alpha=0$ or $\alpha=1$. In order to improve the efficiency of the proposed scheme, we introduce the following cut-off type of hybrid flux,

$$\hat{\mathbf{F}}_{i+1/2} = \begin{cases} \hat{\mathbf{F}}_{i+1/2}^{\text{C}} & 0 \leq \alpha \leq \delta \\ \alpha \hat{\mathbf{F}}_{i+1/2}^{\text{KFVS}} + (1-\alpha) \hat{\mathbf{F}}_{i+1/2}^{\text{C}} & \delta < \alpha < 1-\delta \\ \hat{\mathbf{F}}_{i+1/2}^{\text{KFVS}} & 1-\delta \leq \alpha \leq 1 \end{cases} \quad (10)$$

where $\delta (0 \leq \delta < 0.5)$ is a parameter to control the cut-off range of α . Based on a large number of trials we find that $\delta = 0.02$ is a satisfactory choice after considering the overall performance, such as the accuracy and efficiency, of the proposed scheme, and therefore it is adopted in this paper.

Up to now, we have evaluated all the unknowns in Eq. (10) which can be used to get numerical fluxes for the hybrid kinetic WENO scheme [24]. Although the component by component version of the introduced hybrid kinetic WENO scheme is effective and works reasonably well for many problems, in this paper we will use the more costly, but much more robust characteristic decomposition technique[5] in order to test some demanding problems. The proposed 5th-order/7th-order hybrid kinetic WENO algorithm will be called the W5-HK/W7-HK scheme hereafter in this paper.

3 Numerical experiments

In [24], the 5th order scheme employing the proposed hybrid kinetic approach has been validated. In this section, we will test the 7th order hybrid kinetic WENO scheme in both one-dimensional and two-dimensional cases. The uniform mesh is used for both 1D and 2D test problems.

3.1 Accuracy test

This example is to test the accuracy of the 7th order hybrid kinetic WENO scheme. We solve the 1D Euler equations with the following initial data:

$$\rho(x, 0) = 1 + 0.2 \sin(\pi x), \quad u(x, 0) = 0.7, \quad p(x, 0) = 1. \quad (11)$$

The periodic boundary condition is used, and the computational domain is taken as $[0, 2]$. We compute the solution up to $t=2$. The errors and convergence orders of density are shown in Table 1. This table shows that the 7th order convergence rate can be obtained by both W7-KFVS and W7-HK. Moreover, the W7-HK has smaller absolute errors than the W7-KFVS given the same cell size, this means that the former is more accurate and less dissipative than the latter.

Table 1: 1D accuracy test

| N | Scheme | L^∞ error | order | L^1 error | order | L^2 error | order |
|-----|---------|------------------|-------|-------------|-------|-------------|-------|
| 8 | W7-KFVS | 2.37E-3 | -- | 1.21E-3 | -- | 1.42E-3 | -- |
| | W7-HK | 2.36E-3 | -- | 1.21E-3 | -- | 1.42E-3 | -- |
| 16 | W7-KFVS | 8.35E-5 | 4.83 | 2.99E-5 | 5.34 | 3.87E-5 | 5.20 |
| | W7-HK | 4.14E-5 | 5.83 | 1.97E-5 | 5.94 | 2.32E-5 | 5.94 |
| 32 | W7-KFVS | 1.48E-6 | 5.82 | 4.00E-7 | 6.22 | 5.80E-7 | 6.06 |
| | W7-HK | 5.69E-7 | 6.19 | 2.06E-7 | 6.58 | 2.60E-7 | 6.48 |
| 64 | W7-KFVS | 1.44E-8 | 6.68 | 3.50E-9 | 6.84 | 5.18E-9 | 6.81 |
| | W7-HK | 5.10E-9 | 6.80 | 1.73E-9 | 6.90 | 2.20E-9 | 6.88 |
| 128 | W7-KFVS | 1.19E-10 | 6.92 | 2.84E-11 | 6.95 | 4.20E-11 | 6.95 |
| | W7-HK | 4.09E-11 | 6.96 | 1.39E-11 | 6.96 | 1.76E-11 | 6.97 |

3.2 Blast wave problem

The blast wave problem was originally proposed in [26], which is a challenging test case due to the complex flow structures. The initial flow field is given by

$$(\rho, u, p) = \begin{cases} (1, 0, 1000), & -5 \leq x < -4 \\ (1, 0, 0.01), & -4 \leq x \leq 4 \\ (1, 0, 100), & 4 < x \leq 5 \end{cases} . \quad (12)$$

The computational domain is $[-5, 5]$ with a reflecting boundary condition on both ends. Since the exact solution is unknown for this problem, the reference solution obtained by the W5-HK with 10000 cells is used for comparison. The numerical results with $\Delta x=0.025$ at $t = 0.38$ are shown in Figure 1. From the figure, we can see that the W7-HK/W7-KFVS performs much better than the W5-HK/W5-KFVS. Moreover, the W7-HK performs slightly better than the W7-KFVS, especially for the complex flow regions.

3.3 Shock acoustic-wave interaction

Next we solve the problem proposed by Shu and Osher[3] which describes the interaction of an entropy sine wave with a Mach number 3 right-moving shock. The initial conditions are given by

$$(\rho, u, p) = \begin{cases} (3.857143, 2.629369, 10.333333), & x \leq -4 \\ (1 + 0.2 \sin(5x), 0, 1), & x > -4 \end{cases} \quad (13)$$

The computational domain is $[-5, 5]$, the output time is $t=1.8$. The reference solution for comparison is obtained by the W5-HK with 10000 cells. The numerical results with $\Delta x=0.025$ are shown in Figure 2. From the figure, we can see that the 7th order W7-HK gives much better numerical results than the W5-HK.

3.4 Double Mach reflection problem

This problem was extensively studied in [26] and later by many others. The computational domain is taken as $[0, 4] \times [0, 1]$. Figure 3 displays the close-up of density contours with 30 equally spaced contour lines at $t=0.2$ with a 1920×480 uniform grid. First, it is clearly seen that the 7th order W7-HK/W7-KFVS captures the instability and roll-ups of the slip line better than the 5th order W5-HK/W5-KFVS. Moreover, W7-HK/W5-HK performs slightly better than W7-KFVS/W5-KFVS, which indicates that W7-HK/W5-HK is less dissipative than W7-KFVS/W5-KFVS.

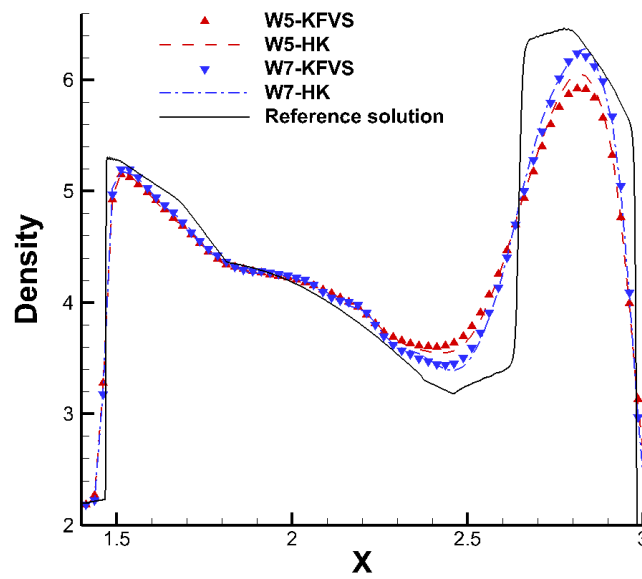
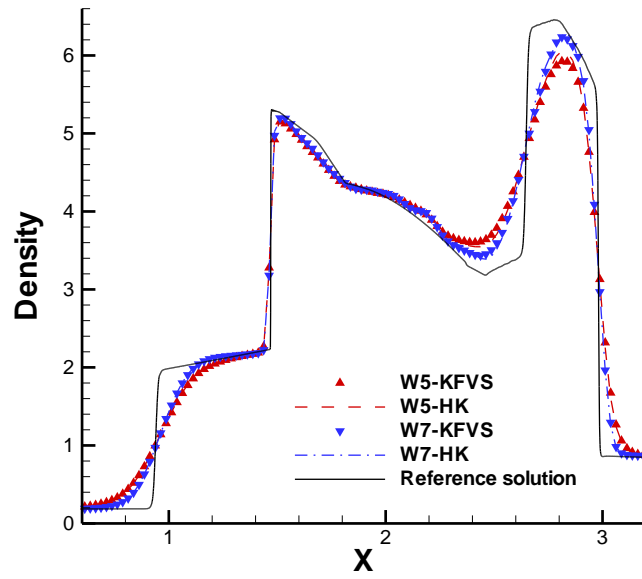


Figure 1: Blast wave problem, the bottom is an enlarged view of the top.

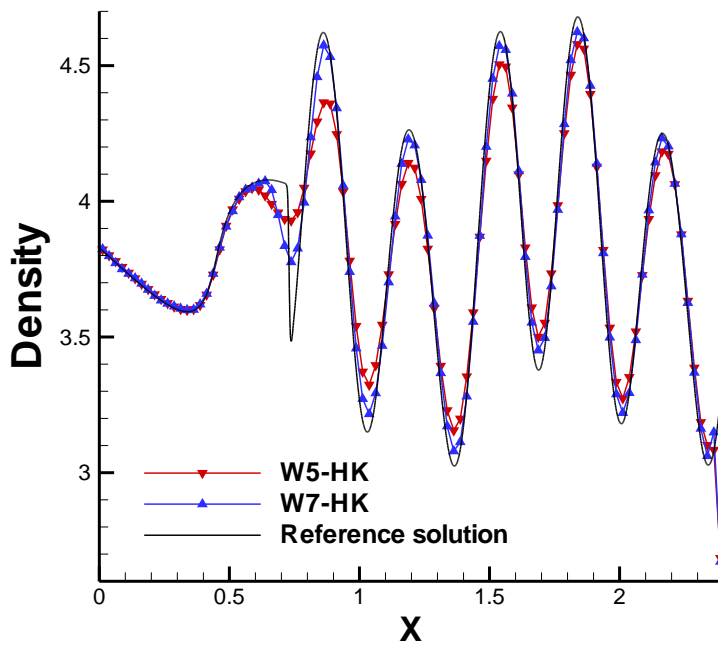
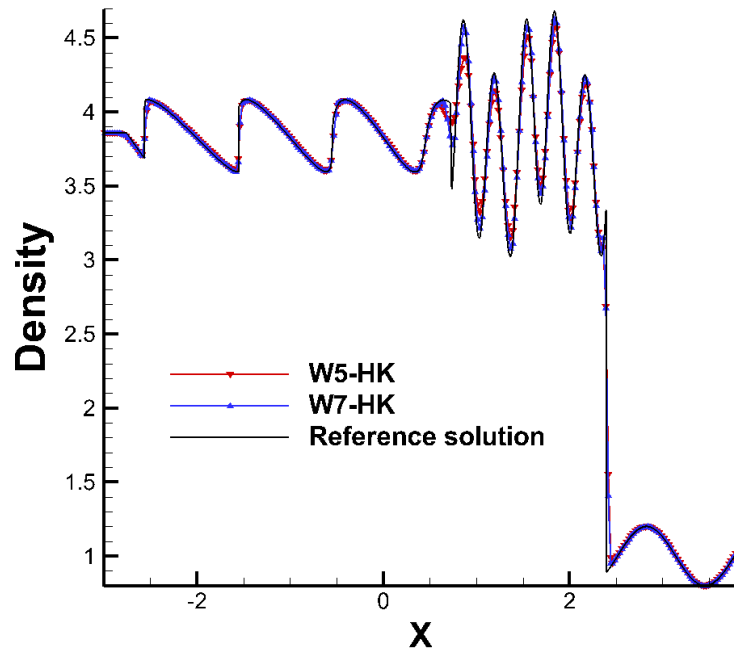


Figure 2: Shock acoustic-wave interaction problem, the bottom is an enlarged view of the top.

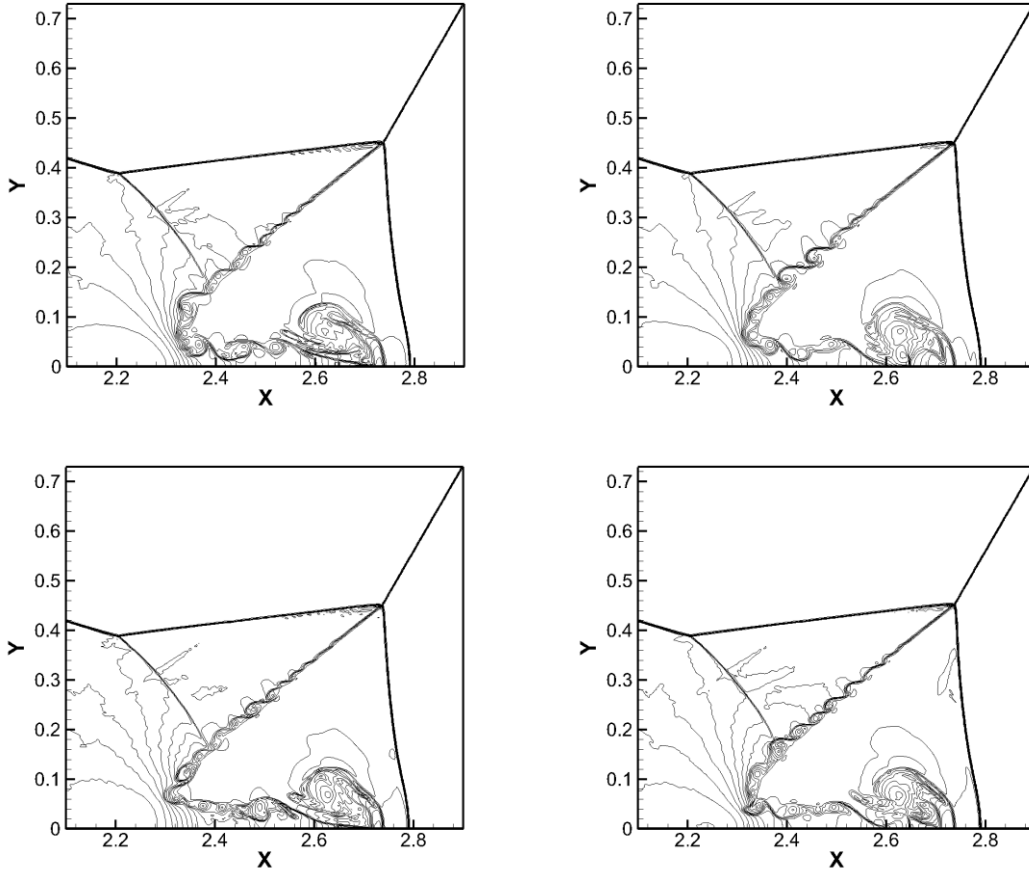


Figure 3: Double Mach reflection problem, $\Delta x = \Delta y = 1/480$. 30 equally spaced density contours from 2 to 22. Top left: W5-KFVS; top right: W5-HK; bottom left: W7-KFVS; bottom right: W7-HK.

4 Conclusions

The hybrid kinetic Weighted Essentially Non-Oscillatory (WENO) scheme proposed in [24] is further studied in this paper. In [24], the 5th order scheme employing the proposed hybrid kinetic approach has been validated, therefore in this paper, we further test the 7th order scheme using the hybrid kinetic method.

Numerical experiments have demonstrated that the present 7th order method (W7-HK) is more accurate and less dissipative than the conventional scheme with the KFVS technique (W7-KFVS) for smooth flows, furthermore the former can provide sharper discontinuity transition than the latter for flows with discontinuities. The present study indicates that the collisionless KFVS technique is intrinsically very dissipative, the cautious consideration of the influences of molecule collisions can really reduce the numerical dissipation of a high-order scheme.

References

- [1] Harten A, Engquist B, Osher S and Chakravarthy S. Uniformly high order essentially non-oscillatory schemes III. *J. Comput. Phys.* 1987; 71: 231-303.
- [2] Shu C-W and Osher S. Efficient implementation of essential nonoscillatory shock capturing schemes. *J. Comput. Phys.* 1988; 77: 439-471.

- [3] Shu C-W and Osher S. Efficient implementation of essential nonoscillatory shock capturing schemes, II. *J. Comput. Phys.* 1989; 83: 32-78.
- [4] Liu X, Osher S and Chan T. Weighted essentially non-oscillatory schemes. *J. Comput. Phys.* 1994; 115: 200-212.
- [5] Jiang G and Shu C-W. Efficient implementation of weighted ENO schemes. *J. Comput. Phys.* 1996; 126: 202-228.
- [6] Pullin DI. Direct simulation methods for compressible inviscid ideal gas flow. *J. Comput. Phys.* 1980; 34: 231-244.
- [7] Mandal JC and Deshpande SM. Kinetic flux vector splitting for Euler equations. *Comput. Fluids* 1994; 23: 447-478.
- [8] Chou SY and Baganoff D. Kinetic flux-vector splitting for the Navier-Stokes equations. *J. Comput. Phys.* 1997; 130: 217-230.
- [9] Xu K. A gas-kinetic BGK scheme for the Navier-Stokes equations and its connection with artificial dissipation and Godunov method. *J. Comput. Phys.* 2001; 171: 289-335.
- [10] Xu K, Mao ML and Tang L. A multidimensional gas-kinetic BGK scheme for hypersonic viscous flow. *J. Comput. Phys.* 2005; 203: 405-421.
- [11] Ohwada T and Kobayashi S. Management of the discontinuous reconstruction in kinetic schemes. *J. Comput. Phys.* 2004; 197: 116-138.
- [12] Li QB, Xu K and Fu S. A high-order gas-kinetic Navier-Stokes solver. *J. Comput. Phys.* 2010; 229: 6715-6731.
- [13] Liu N and Tang H. A high-order accurate gas-kinetic scheme for one and two-dimensional flow simulation. *Commun. Comput. Phys.* 2014; 15: 911-943.
- [14] Kumar G, Girimaji SS and Kerimo J. WENO-enhanced gas-kinetic scheme for direct simulations of compressible transition and turbulence. *J. Comput. Phys.* 2013; 234: 499-523.
- [15] Xuan LJ and Xu K. A new gas-kinetic scheme based on analytical solutions of the BGK equation. *J. Comput. Phys.* 2013; 234: 524-539.
- [16] Luo J and Xu K. A high-order multidimensional gas-kinetic scheme for hydrodynamic equations. *Sci. China Tech. Sci.* 2013; 56: 2370-2384.
- [17] Henrick AK, Aslam TD, Powers JM. Mapped weighted essentially nonoscillatory schemes: Achieving optimal order near critical points. *J. Comput. Phys.* 2005; 207: 542-567.
- [18] Borges R, Carmona M, Costa B, Don WS. An improved weighted essentially non-oscillatory scheme for hyperbolic conservation laws. *J. Comput. Phys.* 2008; 227: 3191-3211.
- [19] Fan P, Shen YQ, Tian BL, Yang C. A new smoothness indicator for improving the weighted essentially non-oscillatory scheme. *J. Comput. Phys.* 2014; 269: 329-354.
- [20] Steger JL and Warming R. Flux vector splitting of the inviscid gas dynamic equation with application to finite difference methods. *J. Comput. Phys.* 1981; 40: 263-293.
- [21] Xu K and Jameson A. Gas-kinetic relaxation (BGK-type) schemes for the compressible Euler equations. AIAA-95-1736, 12th AIAA Computational Fluid Dynamics Conference, 1995.
- [22] Ohwada T and Fukata S. Simple derivation of high-resolution schemes for compressible flows by kinetic approach. *J. Comput. Phys.* 2006; 211: 424-447.
- [23] Liu H and Xu K. A Runge-Kutta discontinuous Galerkin method for viscous flow equations. *J. Comput. Phys.* 2007; 224: 1223-1242.
- [24] Liu H. A hybrid kinetic WENO scheme for inviscid and viscous flows. *Int. J. Numer. Meth. Fluids* 2015; 79:290-305.
- [25] Balsara D S and Shu C W. Monotonicity Preserving Weighted Essentially Non-oscillatory Schemes with Increasingly High Order of Accuracy. *J. Comput. Phys.* 2000; 160: 405-452.
- [26] Woodward P and Colella P. The numerical simulation of two dimensional fluid flow with strong shocks. *J. Comput. Phys.* 1984; 54: 115-173.